Synthesis and Structures of Bis(dithiolene)molybdenum Complexes Related to the Active Sites of the DMSO Reductase Enzyme Family

Booyong S. Lim, James P. Donahue, and R. H. Holm*

Department of Chemistry and Chemical Biology, Harvard University, Cambridge, Massachusetts 02138

Received July 22, 1999

Structural analogues of the reduced (Mo(IV)) sites of members of the DMSO reductase family of molybdoenzymes are sought. These sites usually contain two pterin−dithiolene cofactor ligands and one protein-based ligand. Reaction of $[Mo(MeCN)_3(CO)_3]$ and $[Ni(S_2C_2R_2)_2]$ affords the trigonal prismatic complexes $[Mo(CO)_2(S_2C_2R_2)_2]$ (R = Me (**1**), Ph (**2**)), which by carbonyl substitution serve as useful precursors to a variety of bis(dithiolene)molybdenum(IV,V) complexes. Reaction of **1** with Et_4NOH yields $[MoO(S_2C_2Me_2)_2]^{2-}$ (**3**), which is readily oxidized to $[MoO(S_2C_2Me_2)_2]^{1-}$ (**4**). The hindered arene oxide ligands ArO^- afford the square pyramidal complexes $[Mo(OAr)(S_2C_2R_2)_2]^{1-}$ (**5**, **6**). The ligands PhQ^- afford the trigonal prismatic monocarbonyls $[Mo(CO)(QPh)(S_2C_2Me_2)_2]^{1-}$ (Q = S (**8**), Se (**12**)) while the bulky ligand ArS^- forms square pyramidal $[Mo(SAr)(S_2C_2R_2)_2]^{1-}$ (**9**, **10**). In contrast, reactions with $ArSe^-$ result in $[Mo(CO)(SeAr)(S_2C_2R_2)_2]^{1-}$ (**14**, **15**), which have not been successfully decarbonylated. Other compounds prepared by substitution reactions of **1** and **2** include the bridged dimers $[Mo_2(\mu\text{-}Q)_2(S_2C_2Me_2)_4]^{2-}$ (Q = S (**7**), Se (**11**)) and $[Mo_2(\mu\text{-}SePh)_2(S_2C_2Ph_2)_4]^{2-}$ (**13**). The complexes **1**, **3**−**5**, **7**−**10**, **12**−**14**, $[Mo(S_2C_2Me_2)_3]$ (**16**), and $[Mo(S_2C_2Me_2)_3]^{1-}$ (**17**) were characterized by X-ray structure determinations. Certain complexes approach the binding arrangements in at least one DMSO reductase (**5**/**6**) and its Ser/Cys mutant, and in dissimilatory nitrate reductases (**9**/**10**). This investigation provides the initial demonstration of the new types of bis(dithiolene)molybdenum(IV) complexes available through $[Mo(CO)_2(S_2C_2R_2)_2]$ precursors, some of which will be utilized in reactivity studies. (Ar = 2,6-diisopropylphenyl or 2,4,6-triisopropylphenyl.)

Introduction

Under the Hille classification of molybdenum hydroxylase and oxotransferase enzymes,[1] the DMSO reductase family includes enzymes with two pterin−dithiolene cofactors and a single oxo ligand (or a protonated form) in the oxidized (Mo(VI)) state. Additionally, the enzymes contain one protein-derived ligand at the molybdenum site which varies with enzyme type. The structure of cofactor ligand and demonstrated or probable molybdenum coordination units **a**−**f** in the DMSOR family are shown in Figure 1. Abbreviations used throughout are defined in Chart 1.

Protein crystallography[2] and XAS[3,4] have established the reduced desoxo site $[Mo^{IV}(O{\cdot}Ser)(S_2pd)_2]$ (**a**) and the oxidized monooxo site $[Mo^{VI}O(O{\cdot}Ser)(S_2pd)_2]$ (**b**) for *Rs* DMSO reductase. The serinate ligand (Ser147) occurs in a peptide sequence that is highly conserved in prokaryotic molybdoenzymes. Sequence alignments suggest that the protein ligand may be $Ser{\cdot}O^-$, $Cys{\cdot}S^-$, or $Cys{\cdot}Se^-$ (selenocysteinate) within the enzyme family.[1,2] This possibility has now been confirmed for several enzymes. In dissimilatory *Dd* nitrate reductase, the site $[Mo^{VI}(OH_2)(S{\cdot}Cys)(S_2pd)_2]$ (diprotonated **d**) has been crystallographically identified, and site **c** has been proposed to intervene in the catalytic cycle.[5] Further, site-directed mutagenesis has led to replacement of serinate by cysteinate in *Ec* DMSOR[6] and *Rs* DMSOR,[7] with attendant changes in color, spectroscopic properties, and activity. In the latter enzyme, EXAFS is consistent with Cys147 binding to molybdenum.[4] In formate dehydrogenases, the protein ligand may be cysteinate, as indicated by sequence comparisons,[1,2] or selenocysteinate or a modified version thereof, as detected by crystallography and

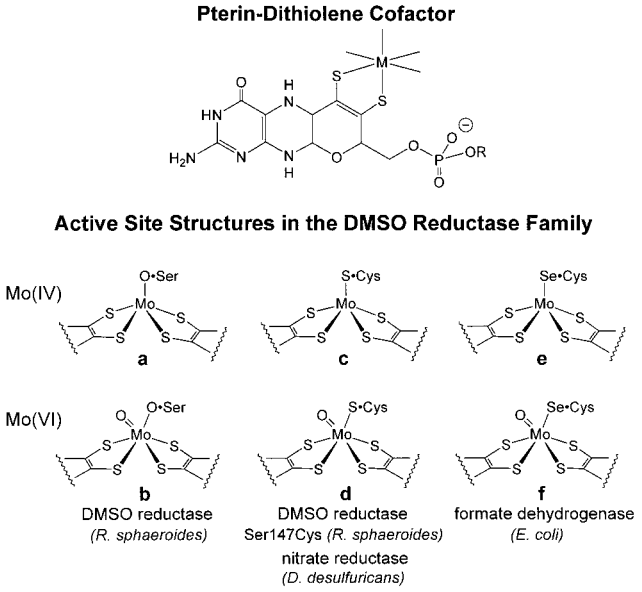

Figure 1. Structures of the pterin−dithiolene cofactor (R absent or a nucleotide) and demonstrated or possible minimal active site structures of enzymes in the DMSOR family. Examples cited are crystallographic results; the oxo ligand may be protonated in certain cases. EXAFS analyses indicate a selenosulfide−thiolate ligand in two FDH enzymes[13,14] (not shown).

(1) Hille, R. *Chem. Rev.* **1996**, *96*, 2757.
(2) Schindelin, H.; Kisker, C.; Hilton, J.; Rajagopalan, K. V.; Rees, D. C. *Science* **1996**, *272*, 1615.
(3) George, G. N.; Hilton, J.; Rajagopalan, K. V. *J. Am. Chem. Soc.* **1996**, *118*, 1113.
(4) George, G. N.; Hilton, J.; Temple, C.; Prince, R. C.; Rajagopalan, K. V. *J. Am. Chem. Soc.* **1999**, *121*, 1256.

10.1021/ic9908672 CCC: $19.00
Published on Web 12/29/1999

Chart 1

$[Mo(CO)_2(S_2C_2Me_2)_2]$	**1**[27]
$[Mo(CO)_2(S_2C_2Ph_2)_2]$	**2**[27]
$[Mo^{IV}O(S_2C_2Me_2)_2]^{2-}$	**3**
$[Mo^{V}O(S_2C_2Me_2)_2]^{1-}$	**4**
$[Mo^{IV}(OC_6H_3\text{-}2,6\text{-}Pr^i_2)(S_2C_2Me_2)_2]^{1-}$	**5**
$[Mo^{IV}(OC_6H_2\text{-}2,4,6\text{-}Pr^i_3)(S_2C_2Ph_2)_2]^{1-}$	**6**
$[Mo^{V}_2(\mu\text{-}S)_2(S_2C_2Me_2)_4]^{2-}$	**7**
$[Mo(CO)(SPh)(S_2C_2Me_2)_2]^{1-}$	**8**
$[Mo^{IV}(SC_6H_2\text{-}2,4,6\text{-}Pr^i_3)(S_2C_2Me_2)_2]^{1-}$	**9**
$[Mo^{IV}(SC_6H_2\text{-}2,4,6\text{-}Pr^i_3)(S_2C_2Ph_2)_2]^{1-}$	**10**
$[Mo^{V}_2(\mu\text{-}Se)_2(S_2C_2Me_2)_4]^{2-}$	**11**
$[Mo(CO)(SePh)(S_2C_2Me_2)_2]^{1-}$	**12**
$[Mo^{IV}_2(\mu\text{-}SePh)_2(S_2C_2Ph_2)_4]^{2-}$	**13**
$[Mo(CO)(SeC_6H_2\text{-}2,4,6\text{-}Pr^i_3)(S_2C_2Me_2)_2]^{1-}$	**14**
$[Mo(CO)(SeC_6H_2\text{-}2,4,6\text{-}Pr^i_3)(S_2C_2Ph_2)_2]^{1-}$	**15**
$[Mo(S_2C_2Me_2)_3]$	**16**[26,27]
$[Mo(S_2C_2Me_2)_3]^{1-}$	**17**

bdt, benzene-1,2-dithiolate(2-), *Dd*, *Desulfovibrio desulfuricans;* DMSOR, dimethyl sulfoxide reductase; *Ec*, *Escherichia coli*; FDH, formate dehydrogenase; mnt, maleonitriledithiolate(2-); qdt, quinoxaline-2,3-dithiolate(2-); $R_2C_2S_2$, generic dithiolene(2-) (including bdt); *Rc*, *Rhodobacter capsulatus;* *Rs*, *Rhodobacter sphaeroides*; S_2pd, pterin-dithiolene cofactor(2-); XAS, X-ray absorption spectroscopy

EXAFS. The sites $[Mo^{IV}(Se{\cdot}Cys)(S_2pd)_2]$ (**e**) in formate-reduced and $[Mo^{VI}(OH)(Se{\cdot}Cys)(S_2pd)_2]$ (monoprotonated **f**) in oxidized *Ec* FDH have been determined by crystallography.[8] However, the EXAFS results for the oxidized and dithionite-reduced forms differ from the X-ray results by revealing a $MoOSeS_4$ coordination unit with an S−Se interaction at 2.19−2.20 Å. This interaction has been suggested as part of a selenosulfide−thiolate ligand (not shown).[9] For *Dd* FDH, EXAFS analysis indicates an oxidized site essentially the same as that deduced for the *Ec* enzyme by the same method and a dithionite-reduced site $[Mo^{IV}(OH_2)(Se{\cdot}Cys)(S_2pd)_2]$ lacking the Se−S interaction[10] (**e** with an additional water ligand).

While highly significant advances have been made recently in defining structures and developing structure−function relationships of molybdoenzymes,[2,11−15] there remain unresolved problems, or at the very least unexpected observations, in the DMSOR family. These include unsymmetrical pterin−dithiolene ligand coordination and different binding modes in oxidized and reduced enzymes in the crystalline state[2] compared to the tight symmetrical chelation deduced from EXAFS[3,4] and resonance Raman[16] spectroscopy in solution and apparent lack of agreement in crystal structures of the same[17−19] and closely related[2,17] enzymes and in crystallographic and EXAFS structures of the same enzyme.[8,9] These complications notwithstanding, there are regularities. Members of this family possess a monooxo or monohydroxo oxidized site and a desoxo reduced site with a protein ligand in each. The oxotransferase members operate by the minimal reaction $Mo^{IV} + XO \rightleftarrows Mo^{VI}O + X$, where XO and X are either substrate or product, a matter demonstrated by isotope labeling[20] and resonance Raman spectroscopy.[16]

Historically, the chemistry of molybdenum dithiolenes has been dominated by the synthesis and study of two types of molecules: the square pyramidal oxobis(dithiolenes) $[MoO(S_2C_2R_2)_2]^{2-,1-}$ [21−24] and the tris(dithiolenes) $[Mo(S_2C_2R_2)_3]^{2-,1-,0}$.[25−27] (Extensive citations to work on these species are available elsewhere.[24]) In pursuing the chemistry of bis(dithiolenes), it is desirable to determine what species are accessible and what structures they adopt, prior to development of reactivity properties. Given the range of structural possibilities for oxidized and reduced sites, basic representations of which are set out in Figure 1, we directed our attention toward the synthesis and property elucidation of analogue molecules. In this work, we have concentrated on bis(dithiolene)molybdenum(IV) species with varying axial ligation intended to approach the situation represented by sites **a**, **c**, and **e**. This investigation is a continuation of our exploration of biologically relevant bis(dithiolene)molybdenum complexes.[23,24,28] In this context, we note related contributions by others on $Mo^{IV}O$ systems.[21,22]

Experimental Section

Preparation of Compounds. All reactions and manipulations were conducted under a pure dinitrogen atmosphere using either an inert atmosphere box or standard Schlenk techniques. Acetonitrile and dichloromethane were freshly distilled from CaH_2, and methanol was distilled from magnesium; CD_3CN and DMF (Aldrich) were dried over freshly activated molecular sieves. Ether and THF were distilled from sodium/benzophenone and stored over 4 Å molecular sieves. In the following preparations, all volume reduction and evaporation steps were performed in vacuo. The compounds $(Et_4N)(OC_6H_3\text{-}2,6\text{-}Pr^i_2)$, $(Et_4N)(OC_6H_2\text{-}2,4,6\text{-}Pr^i_3)$, $(Et_4N)(SC_6H_2\text{-}2,4,6\text{-}Pr^i_3)$, (Et_4N)(SePh), and (Et_4N)-

(5) Dias, J. M.; Than, M. E.; Humm, A.; Huber, R.; Bourenkov, G. P.; Bartunik, H. D.; Bursakov, S.; Calvete, J.; Caldeira, J.; Carneiro, C.; Moura, J. J. G.; Moura, I.; Romão, M. J. *Structure* **1999**, *7*, 65.
(6) Trieber, C. A.; Rothery, R. A.; Weiner, J. H. *J. Biol. Chem.* **1996**, *271*, 27339.
(7) Hilton, J. C.; Temple, C. A.; Rajagopalan, K. V. *J. Biol. Chem.* **1999**, *274*, 8428.
(8) Boyington, J. C.; Gladyshev, V. N.; Khangulov, S. V.; Stadtman, T. C.; Sun, P. D. *Science* **1997**, *275*, 1305.
(9) George, G. N.; Colangelo, C. M.; Dong, J.; Scott, R. A.; Khangulov, S. V.; Gladyshev, V. N.; Stadtman, T. C. *J. Am. Chem. Soc.* **1998**, *120*, 1267.
(10) George, G. N.; Costa, C.; Moura, J. J. G.; Moura, I. *J. Am. Chem. Soc.* **1999**, *121*, 2625.
(11) Hille, R. *J. Biol. Inorg. Chem.* **1996**, *1*, 397.
(12) Kisker, C.; Schindelin, H.; Rees, D. C. *Annu. Rev. Biochem.* **1997**, *66*, 233.
(13) Romão, M. J.; Knäblein, J.; Huber, R.; Moura, J. J. G. *Prog. Biophys. Mol. Biol.* **1997**, *68*, 121.
(14) Romão, M. J.; Huber, R. *Struct. Bonding* **1998**, *90*, 69.
(15) Hille, R.; Rétey, J.; Bartlewski-Hof, U.; Reichenbecher, W.; Schink, B. *FEMS Microbiol. Rev.* **1999**, *22*, 489.
(16) Garton, S. D.; Hilton, J.; Oku, H.; Crouse, B. R.; Rajagopalan, K. V.; Johnson, M. K. *J. Am. Chem. Soc.* **1997**, *119*, 12906.
(17) McAlpine, A. S.; McEwan, A. G.; Shaw, A. L.; Bailey, S. *J. Biol. Inorg. Chem.* **1997**, *2*, 690.
(18) McAlpine, A. S.; McEwan, A. G.; Bailey, S. *J. Mol. Biol.* **1998**, *275*, 613.
(19) Schneider, F.; Löwe, J.; Huber, R.; Schindelin, H.; Kisker, C.; Knäblein, J. *J. Mol. Biol.* **1996**, *263*, 53. In this structure of *Rc* DMSOR, the oxidized site is $[MoO_2(O{\cdot}Ser)(S_2pd)]$. The second pterin−dithiolene cofactor molecule is not coordinated (Mo···S = 3.5, 3.9 Å).
(20) Schultz, B. E.; Hille, R.; Holm, R. H. *J. Am. Chem. Soc.* **1995**, *117*, 827.
(21) Oku, H.; Ueyama, N.; Kondo, M.; Nakamura, A. *Inorg. Chem.* **1994**, *33*, 209.
(22) Davies, E. S.; Beddoes, R. L.; Collison, D.; Dinsmore, A.; Docrat, A.; Joule, J. A.; Wilson, C. R.; Garner, C. D. *J. Chem. Soc., Dalton Trans.* **1997**, 3985.
(23) Donahue, J. P.; Lorber, C.; Nordlander, E.; Holm, R. H. *J. Am. Chem. Soc.* **1998**, *120*, 3259.
(24) Donahue, J. P.; Goldsmith, C. R.; Nadiminti, U.; Holm, R. H. *J. Am. Chem. Soc.* **1998**, *120*, 12869.
(25) McCleverty, J. A. *Prog. Inorg. Chem.* **1968**, *10*, 49.
(26) Schrauzer, G. N.; Mayweg, V. P. *J. Am. Chem. Soc.* **1966**, *88*, 3235.
(27) Schrauzer, G. N.; Mayweg, V. P.; Heinrich, W. *J. Am. Chem. Soc.* **1966**, *88*, 5174.
(28) Tucci, G. C.; Donahue, J. P.; Holm, R. H. *Inorg. Chem.* **1998**, *37*, 1602.

Table 1. Crystallographic Data[a] for **1** and Compounds Containing **3**−**5**

	1	$(Et_4N)_2$[**3**]	(Et_4N)[**4**]	(Et_4N)[**5**]
empirical formula	$C_{10}H_{12}MoO_2S_4$	$C_{24}H_{52}MoN_2OS_4$	$C_{16}H_{32}MoNOS_4$	$C_{28}H_{49}MoNOS_4$
fw	388.38	608.86	478.61	639.86
cryst syst	triclinic	monoclinic	tetragonal	monoclinic
space group	$P\bar{1}$	$P2_1/c$	$I\bar{4}2d$	$P2_1/c$
Z	2	4	8	8
a, Å	7.0975(2)	13.110(1)	12.7822(1)	18.334(2)
b, Å	7.7209(2)	13.979(2)	12.7822(1)	19.919(3)
c, Å	13.7181(3)	16.694(1)	27.3827(3)	17.809(2)
α, deg	93.586(1)			
β, deg	94.123(1)	94.558(7)		90.099(3)
γ, deg	95.551(1)			
V, Å^3	744.45(3)	3049.7(5)	4473.91(7)	6504(2)
d_{calcd}, g/cm^3	1.733	1.326	1.421	1.307
μ, mm^{-1}	1.428	0.722	0.963	0.681
2θ range, deg	3-56	3-56	3-56	3-45
GOF(F^2)	1.027	1.089	1.090	1.020
R1[b] (wR2[c]), %	2.56 (6.38)	3.01 (7.68)	3.53 (5.67)	6.09 (13.61)

[a] Obtained at 213 K with graphite-monochromatized Mo Kα (λ = 0.710 73 Å) radiation. [b] $R1 = \sum||F_o| - |F_c||/\sum|F_o|$. [c] $wR2 = \{\sum[w(F_o^2 - F_c^2)^2/\sum w(F_o^2)^2]\}^{1/2}$.

Table 2. Crystallographic Data[a] for Compounds Containing **7**−**10**

	$(Ph_4P)_2$[**7**]·2DMF	(Bu_4N)[**8**]	(Et_4N)[**9**]	(Et_4N)[**10**]
empirical formula	$C_{70}H_{78}Mo_2N_2O_2P_2S_{10}$	$C_{31}H_{53}MoNOS_5$	$C_{31}H_{55}MoNS_5$	$C_{51}H_{63}MoNS_5$
fw	1553.76	711.98	698.00	946.26
cryst syst	monoclinic	monoclinic	monoclinic	monoclinic
space group	$P2_1/c$	$P2_1/c$	$C2/c$	$P2_1/c$
Z	2	4	8	4
a, Å	14.9620(3)	9.558(1)	35.3419(2)	18.405(2)
b, Å	16.0040(3)	19.684(2)	15.3984(3)	15.255(1)
c, Å	15.915(2)	19.248(2)	15.1147(2)	19.465(2)
β, deg	107.942(1)	98.081(7)	113.582(1)	113.314(6)
V, Å^3	3625.5(1)	3585.3(7)	7538.6(2)	5019.2(8)
d_{calcd}, g/cm^3	1.423	1.319	1.230	1.252
μ, mm^{-1}	0.723	0.681	0.644	0.502
2θ range, deg	3-56	3-56	3-45	3-56
GOF(F^2)	1.029	1.077	1.075	1.026
R1[b] (wR2[c]), %	3.95(5.88)	4.40(6.86)	3.16(7.11)	3.81(7.24)

[a] Obtained at 213 K with graphite-monochromatized Mo Ka (λ = 0.710 73 Å) radiation. [b] $R1 = \sum||F_o| - |F_c||/\sum|F_o|$. [c] $wR2 = \{\sum[w(F_o^2 - F_c^2)^2/\sum w(F_o^2)^2]\}^{1/2}$.

(SeC_6H_2-2,4,6-Pr^i_3) were prepared from the corresponding phenol, thiol, or selenol by the method for $(Et_4N)(SPh)$.[29] The compounds 2,4,6-$Pr^i_3C_6H_2SH$[30] and 2,4,6-$Pr^i_3C_6H_2SeH$[31] were obtained by published methods. The identities of 13 of the compounds whose syntheses are described were confirmed by X-ray structure determinations (Tables 1−3).

2,4,6-Triisopropylphenol. The following method is much more convenient than published multistep high-temperature procedures. At −78 °C, a solution of 5.0 g (18 mmol) of 1-bromo-2,4,6 triisopropylbenzene in 100 mL of THF was treated with 21 mL (36 mmol) of 1.7 M Bu^tLi in pentane, and the reaction mixture was stirred for 3 h. Dioxygen was bubbled through the solution as it was allowed to warm to room temperature overnight. To the resulting pale yellow solution was added 100 mL of a saturated aqueous Et_4NCl solution. THF and pentane were removed, leaving an organic layer on the aqueous phase. The mixture was extracted with ether (3 × 50 mL), the ether was evaporated, and the residue was chromatographed on silica gel with 9:1 hexane/ether. The product was obtained as 3.0 g (77%) of a pale yellow liquid whose NMR spectrum is consistent with that of the compound prepared by a different method.[32] ^{1}H NMR ($CDCl_3$): δ 1.39 (d, 6), 1.41 (d, 12), 3.00 (septet, 1), 3.31 (septet, 2), 4.90 (s, 1), 7.08 (s, 2).

$[Mo(CO)_2(S_2C_2Me_2)_2]$. This procedure leads to higher yields than that originally reported[27] and is analogous to our improved procedure for $[W(CO)_2(S_2C_2Me_2)_2]$.[33] A mixture of 2.00 g (6.60 mmol) of $[Mo(CO)_3(MeCN)_3]$[34] and 4.00 g (13.6 mmol) of $[Ni(S_2C_2Me_2)_2]$[35] was dissolved in 1 L of dichloromethane. The reaction mixture was stirred for 2 d, resulting in a dark violet color, and was filtered. The filtrate was reduced to dryness and the solid violet residue was twice chromatographed on silica gel using 4:1 pentane/benzene (v/v). Removal of solvent afforded the product as 0.770 g (30%) of a dark red-violet microcrystalline solid. IR (Nujol): ν_{CO} 2025, 1964 cm^{-1}. ^{1}H NMR (CD_3CN): δ 2.88 (s). Absorption spectrum (acetonitrile/THF, 5:1 v/v): λ_{max} (ϵ_M) 389 (5660), 529 (10 600), 647 (sh, 1140) nm. The absorption spectrum is in satisfactory agreement with that reported earlier.[27]

$[Mo(CO)_2(S_2C_2Ph_2)_2]$. The preceding method was followed but with use of $[Ni(S_2C_2Ph_2)_2]$.[35] The product was obtained as a blue-violet solid (31% yield) after silica gel chromatography with 7:3 *n*-pentane/benzene (v/v). IR (Nujol): ν_{CO} 2032, 1983 cm^{-1}. Absorption spectrum (THF): λ_{max} (ϵ_M) 402 (6240), 561 (14 400), 690 (1640), 847 (415) nm. Comparison of the absorption spectrum with that previously reported[27] confirmed the identity of the compound.

$(Et_4N)_2[MoO(S_2C_2Me_2)_2]$. A solution of 83 mg (0.21 mmol) of $[Mo(CO)_2(S_2C_2Me_2)_2]$ in 3 mL of THF was treated with 277 μL (0.41 mmol) of a 25% solution of Et_4NOH in methanol. The violet solution became blue immediately with accompanying vigorous gas evolution. The reaction mixture was stirred overnight, leading to the formation of a

(29) Palermo, R. E.; Power, P. P.; Holm, R. H. *Inorg. Chem.* **1982**, *21*, 173.
(30) Blower, P. J.; Dilworth, J. R.; Hutchinson, J. P.; Zubieta, J. A. *J. Chem. Soc., Dalton Trans.* **1985**, 1533.
(31) Bochmann, M.; Webb, K. J.; Hursthouse, M. B.; Mazid, M. *J. Chem. Soc., Dalton Trans.* **1991**, 2317.
(32) Klemm, L. H.; Taylor, D. R. *J. Org. Chem.* **1980**, *45*, 4326.
(33) Goddard, C. A.; Holm, R. H. *Inorg. Chem.* **1999**, *38*, 5389.
(34) Tate, D. P.; Knipple, W. R.; Augl, J. M. *Inorg. Chem.* **1962**, *1*, 433.
(35) Schrauzer, G. N.; Mayweg, V. P. *J. Am. Chem. Soc.* **1965**, *87*, 1483.

Table 3. Crystallographic Data[a] for **16** and Compounds Containing **12**−**14** and **17**

	(Bu_4N)[**12**]	$(Et_4N)_2$[**13**]·2MeCN·Et_2O	(Et_4N)[**14**]	**16**	(Et_4N)[**17**]·MeCN
empirical formula	$C_{31}H_{53}MoNOS_4Se$	$C_{92}H_{106}Mo_2N_4OS_8Se_2$	$C_{32}H_{55}MoNOS_4Se$	$C_{12}H_{18}MoS_6$	$C_{22}H_{41}MoN_2S_6$
fw	758.88	1890.09	772.91	450.56	621.87
cryst syst	monoclinic	monoclinic	orthorhombic	triclinic	monoclinic
space group	$P2_1/c$	$P2_1/c$	$Pbcn$	$P\bar{1}$	$P2_1/n$
Z	4	4	8	2	4
a, Å	9.476(3)	11.609(3)	25.5665(7)	7.0301(3)	9.619(1)
b, Å	19.967(4)	29.27(1)	16.8041(5)	8.9791(3)	24.149(3)
c, Å	19.285(6)	26.953(8)	17.1866(5)	14.8274(5)	13.256(2)
α, deg				83.99(1)	
β, deg	97.75(3)	101.23(2)		81.602(2)	105.35(1)
γ, deg				72.108(2)	
V, Å^3	3616(2)	8982(5)	7383.7(4)	879.36(6)	2970.4(7)
d_{calcd}, g/cm^3	1.394	1.398	1.391	1.702	1.391
μ, mm^{-1}	1.624	1.323	1.592	1.442	0.877
2θ range, deg	3-45	3-45	3-56	3-56	3-45
GOF(F^2)	1.050	1.090	1.000	0.951	1.025
R1[b] (wR2[c]), %	5.35(8.06)	4.42(8.00)	5.35(8.06)	4.99(9.99)	4.38(11.61)

[a] Obtained at 213 K with graphite-monochromatized Mo Kα (λ = 0.710 73 Å) radiation. [b] $R1 = \sum||F_o| - |F_c||/\sum|F_o|$. [c] $wR2 = \{\sum[w(F_o^2 - F_c^2)^2/\sum w(F_o^2)^2]\}^{1/2}$.

mixture of yellow-brown and green-blue solids. This material was collected by filtration and dissolved in a minimal volume of acetonitrile to give a yellow-green solution. Several volume equivalents of ether were introduced by vapor diffusion; upon standing, a mixture of large orange-brown and needlelike green-blue crystals formed. The mixture was collected and washed with acetonitrile (2 × 0.5 mL) and ether (2 mL) to remove the green-blue component. The remaining solid was recrystallized from acetonitrile/ether to afford the product as 60 mg (47%) of orange-brown crystals. IR (Nujol): ν_{MoO} 889 cm^{-1}. ^{1}H NMR (CD_3CN, anion): δ 2.16 (s). Absorption spectrum (acetonitrile): λ_{max} (ϵ_M) 259 (sh, 12 600), 300 (4680), 463 (184), 834 (130) nm. Anal. Calcd for $C_{24}H_{52}MoN_2OS_4$: C, 47.34; H, 8.61; N, 4.60; S, 21.06. Found: C, 47.29; H, 8.43; N, 4.66; S, 21.00. The green-blue byproduct has been identified as $(Et_4N)_2[Mo(CO)_2(S_2C_2Me_2)_2]$.[36]

(Et_4N)[$MoO(S_2C_2Me_2)_2$]. A solution of 50 mg (0.082 mmol) of $(Et_4N)_2[MoO(S_2C_2Me_2)_2]$ in 2 mL of acetonitrile was treated with a solution of 11 mg (0.043 mmol) of iodine in 0.5 mL of THF. The resulting blue-violet solution was stirred for 2 h, and the solvent was removed to give a dark blue-violet solid. The material was dissolved in a minimal volume of THF, the solution was filtered, and several volume equivalents of ether were introduced into the filtrate by vapor diffusion. The product was collected by filtration as 24 mg (61%) of violet crystals. IR (Nujol): ν_{MoO} 910 cm^{-1}. Absorption spectrum (acetonitrile/THF, 1:1 v/v): λ_{max} (ϵ_M) 280 (5360), 363 (1330), 575 (560), 826 (1680). Anal. Calcd for $C_{16}H_{32}MoNOS_4$: C, 40.15; H, 6.74; N, 2.93; S, 26.80. Found: C, 40.19; H, 6.73; N, 2.98; S, 26.93.

(Et_4N)[$Mo(OC_6H_3$-2,6-$Pr^i_2)(S_2C_2Me_2)_2$]. A solution of 51 mg (0.17 mmol) of (Et_4N)(OC_6H_3-2,6-Pr^i_2) in 1 mL of acetonitrile was added to a suspension of 54 mg (0.14 mmol) of $[Mo(CO)_2(S_2C_2Me_2)_2]$ in 1 mL of acetonitrile. The reaction mixture was stirred overnight, generating a brown solution which was filtered. The filtrate was reduced to dryness, the solid residue was dissolved in a minimal volume of THF, and several volume equivalents of ether were added. The solution was allowed to stand overnight, during which the product separated as 45 mg (50%) of orange-brown crystals. ^{1}H NMR (CD_3CN, anion): δ 0.97 (d, 12), 2.49 (s, 12), 3.14 (septet, 2), 6.71 (t, 1), 6.79 (d, 2). Absorption spectrum (THF): λ_{max} (ϵ_M) 260 (12 600), 336 (12 400), 411 (3900), 475 (sh, 1630), 567 (530), 724 (160) nm.

(Et_4N)[$Mo(OC_6H_2$-2,4,6-$Pr^i_3)(S_2C_2Ph_2)_2$]. The preceding method was followed but with use of $[Mo(CO)_2(S_2C_2Ph_2)_2]$ and (Et_4N)(OC_6H_2-2,4,6-Pr^i_3). The product was isolated as a red-brown crystalline solid (66%). ^{1}H NMR (THF-d_8, anion): δ 1.04 (d, 12), 1.14 (d, 6), 2.71 (m, 2), 3.22 (m, 1), 6.65 (s, 2), 7.05−7.40 (m, 20). Absorption spectrum (THF): λ_{max} (ϵ_M) 322 (sh, 20 800), 348 (31 900), 413 (sh, 5980), 460 (sh, 1800), 544 (620), 790 (310) nm. Anal. Calcd for $C_{51}H_{63}MoNOS_4$: C, 65.85; H, 6.83; N, 1.51; S, 13.79. Found: C, 65.75; H, 6.94; N, 1.52; S, 13.72.

(36) Femitchev, D.; Lim, B. S.; Holm, R. H. Results to be published.

(Ph_4P)$_2$[$Mo_2(\mu$-S)$_2(S_2C_2Me_2)_4$]·2DMF. A suspension of Na_2S (12 mg, 0.15 mmol) in 3 mL of acetonitrile was added to a solution of 58 mg (0.15 mmol) of $[Mo(CO)_2(S_2C_2Me_2)_2]$ in 10 mL of acetonitrile. The reaction mixture was stirred for 3 h, during which the color changed from deep violet to blue-gray. Solvent was removed, and the solid residue was added to a solution of 128 mg (0.31 mmol) of Ph_4PBr in 5 mL of acetonitrile. The mixture was stirred for 15 min, filtered, and allowed to stand for 3 h. A blue-gray solid was collected, washed with acetonitrile (3 × 3 mL), and dissolved in a minimal volume of DMF. Several volume equivalents of ether were introduced by vapor diffusion over several days. The product was obtained as 21 mg (19%) of a dark green-blue crystalline solid. Absorption spectrum (DMF): λ_{max} (ϵ_M) 274 (15 000), 293 (11 000), 381 (6900), 459 (5700), 577 (6900), 731 (6300) nm.

(Bu_4N)[$Mo(CO)(SPh)(S_2C_2Me_2)_2$]. This compound was prepared using PhSSPh by a procedure analogous to the method for (Bu_4N)-$[Mo(CO)(SePh)(S_2C_2Me_2)_2]$ (vide infra). The product was isolated as dark green-brown crystals (53%). IR (Nujol): ν_{CO} 1961 cm^{-1}. ^{1}H NMR (CD_3CN, anion): δ 2.54 (s, 12), 7.02 (t, 1), 7.10 (t, 2), 7.30 (d, 2). Absorption spectrum (acetonitrile): λ_{max} (ϵ_M) 295 (8290), 377 (5230), 470 (6330), 625 (2090) nm. Anal. Calcd for $C_{31}H_{53}MoNOS_5$: C, 52.29; H, 7.50; N, 1.97; S, 22.52. Found: C, 52.11; H, 7.43; N, 1.91; S, 22.40.

(Et_4N)[$Mo(CO)(SPh)(S_2C_2Me_2)_2$]. This compound was prepared using (Et_4N)(SPh)[29] by a procedure analogous to the method for (Et_4N)-$[Mo(CO)(SePh)(S_2C_2Me_2)_2]$ (vide infra). The residue from the filtrate after washing was dissolved in a minimal volume of THF, and several volume equivalents of ether were added. The product was isolated as a dark green-brown microcrystalline solid (60%). IR (Nujol): ν_{CO} 1942 cm^{-1}. The absorption and ^{1}H NMR spectra of the anion are identical to those of the Bu_4N^+ salt.

(Et_4N)[$Mo(SC_6H_2$-2,4,6-$Pr^i_3)(S_2C_2Me_2)_2$]. A solution of 66 mg (0.18 mmol) of (Et_4N)(SC_6H_2-2,4-6-Pr^i_3) in 1 mL of THF was added to a solution of 70 mg (0.18 mmol) of $[Mo(CO)_2(S_2C_2Me_2)_2]$ in 1 mL of THF. The resulting green-brown solution was stirred for 2 h and filtered. The filtrate was slowly reduced to dryness to give a red-brown solid, which was dissolved in a minimal volume of THF. Several volume equivalents of ether were added, and the solution was allowed to stand overnight. The product was isolated as 85 mg (68%) of red-brown crystals. ^{1}H NMR (THF-d_8, anion): δ 1.06 (d, 12), 1.22 (d, 6), 2.58 (s, 12), 2.73 (m, 1), 3.74 (m, 2), 6.65 (s, 2). Absorption spectrum (THF): λ_{max} (ϵ_M) 270 (9250), 330 (6390), 378 (sh, 3970), 417 (sh, 2440), 478 (sh, 1650), 548 (sh, 1240), 727 (330) nm. Anal. Calcd for $C_{31}H_{55}MoNS_5$: C, 53.34; H, 7.94; N, 2.01; S, 22.97. Found: C, 53.78; H, 8.01; N, 2.03; S, 22.79.

(Et_4N)[$Mo(SC_6H_2$-2,4,6-$Pr^i_3)(S_2C_2Ph_2)_2$]. The preceding method was followed but with use of $[Mo(CO)_2(S_2C_2Ph_2)_2]$. The product was obtained as red-brown crystals (74%). ^{1}H NMR (THF-d_8, anion): δ 1.07 (d, 12), 1.19 (d, 6), 2.79 (m, 1), 3.91 (m, 2), 6.77 (s, 2), 7.05 (t, 4), 7.11 (t, 8), 7.33 (d, 8). Absorption spectrum (THF): λ_{max} (ϵ_M) 330

(10 800), 358 (sh, 9400), 381 (6460), 411 (sh, 3900), 473 (sh, 2040), 549 (1450), 748 (558) nm. Anal. Calcd for $C_{51}H_{63}MoNS_5$: C, 64.73; H, 6.71; N, 1.48; S, 16.94. Found: C, 64.64; H, 6.65; N, 1.48; S, 16.86.

$(Ph_4P)_2[Mo_2(\mu\text{-}Se)_2(S_2C_2Me_2)_4]\cdot 2DMF$. The procedure for $(Ph_4P)_2[Mo_2(\mu\text{-}S)_2(S_2C_2Me_2)_4]\cdot 2DMF$ was followed but with use of Li_2Se. The product was obtained as dark green crystals (17%). Absorption spectrum (DMF): λ_{max} (ϵ_M) 276 (21 000), 291 (13 000), 391 (7100), 459 (8600), 619 (6800), 753 (6900) nm. The compound was identified by its isomorphous relationship to $(Ph_4P)_2[Mo_2(\mu\text{-}S)_2(S_2C_2Me_2)_4]\cdot 2DMF$ (Table 2): monoclinic, $P2_1/c$, $a = 15.00(4)$ Å, $b = 15.89(4)$ Å, $c = 15.98(4)$ Å, $\beta = 108.19(3)°$, $V = 3621(1)$ Å^3.

$(Bu_4N)[Mo(CO)(SePh)(S_2C_2Me_2)_2]$. A solution of 26 mg (0.083 mmol) of diphenyl diselenide was treated with 169 μL (0.17 mmol) of a 1 M solution of $LiBHEt_3$ in THF. Gas evolution accompanied an immediate color change from pale yellow to colorless. The solution was stirred for 30 min and was added to a dark violet solution of 56 mg (0.14 mmol) of $[Mo(CO)_2(S_2C_2Me_2)_2]$ in 1 mL of THF. The reaction mixture became green-brown within 1 min and was stirred for 2 h. A solution of 54 mg (0.14 mmol) of $(Bu_4N)(PF_6)$ in 1 mL of THF was added; the reaction mixture was stirred for 10 min. Removal of solvent left a sticky residue, which upon washing with ether (2×5 mL) and hexane (5 mL) gave a black solid. This material was dissolved in the minimum volume of acetonitrile, and several volume equivalents of ether were added to the solution, which was allowed to stand overnight. Solvent was decanted from a crystalline solid, which was washed with ether to afford the product as 74 mg (70%) of a dark green-brown crystalline solid. IR (Nujol): ν_{CO} 1956 cm^{-1}. ^{1}H NMR (CD_3CN, anion): δ 2.56 (s, 12), 6.96 (m, 3), 7.18 (m, 2). Absorption spectrum (acetonitrile): λ_{max} (ϵ_M) 306 (11 500), 377 (6440), 473 (8260), 615 (2930), 802 (1070) nm. Anal. Calcd for $C_{31}H_{53}MoNOS_4Se$: C, 49.06; H, 7.04; N, 1.85; S, 16.90; Se, 10.40. Found: C, 48.96; H, 7.08; N, 1.78; S, 16.69; Se, 10.07.

$(Et_4N)[Mo(CO)(SePh)(S_2C_2Me_2)_2]$. A solution of 40 mg (0.14 mmol) of $(Et_4N)(SePh)$ in 1 mL of acetonitrile was added to a suspension of 51 mg (0.13 mmol) of $[Mo(CO)_2(S_2C_2Me_2)_2]$ in 1 mL of acetonitrile. The dark green solution which formed within 1 min was stirred for 2 h and filtered. The filtrate was reduced in volume until an oily residue formed. The material was washed with ether (2×5 mL) and hexane (5 mL) and dissolved in a minimum volume of acetonitrile. The product was obtained as in the preceding preparation as 67 mg (80%) of dark green-brown crystals. IR (Nujol): ν_{CO} 1945 cm^{-1}. The absorption and ^{1}H NMR spectra of the anion are identical to those of the Bu_4N^+ salt.

$(Et_4N)_2[Mo_2(\mu\text{-}SePh)_2(S_2C_2Ph_2)_4]\cdot {}^1/_2MeCN$. A solution of 24 mg (0.084 mmol) of $(Et_4N)(SePh)$ in 1 mL of acetonitrile was added to a solution of 54 mg (0.085 mmol) of $[Mo(CO)_2(S_2C_2Ph_2)_2]$ in 1 mL of THF. The brown reaction mixture was stirred for 2 h in the dark. The oily brown residue obtained after removal of solvent was washed with ether (3×5 mL) and dissolved in a minimal volume of acetonitrile. Several volume equivalents of ether were added to the solution, which was allowed to stand overnight. The product was obtained as 59 mg (79%) of brown needlelike crystals. ^{1}H NMR (CD_3CN, anion): δ 7.0−8.4 (m). Absorption spectrum (acetonitrile): λ_{max} (ϵ_M) 270 (sh, 95 400), 358 (sh, 33 000), 416 (sh, 20 500), 548 (9320), 670 (sh, 4380) nm. The product gave an acceptable analysis as the acetonitrile hemisolvate. Anal. Calcd. for $C_{84}H_{90}Mo_2N_2S_8Se_2\cdot {}^1/_2C_2H_3N$: C, 58.19; H, 5.28; N, 2.00; S, 14.62; Se, 9.00. Found: C, 58.29; H, 5.46; N, 2.32; S, 14.84; Se, 9.03.

$(Et_4N)[Mo(CO)(SeC_6H_2\text{-}2,4,6\text{-}Pr^i_3)(S_2C_2Me_2)_2]$. A solution of 78 mg (0.19 mmol) of $(Et_4N)(SeC_6H_2\text{-}2,4,6\text{-}Pr^i_3)$ in 1 mL of acetonitrile was added to a solution of 75 mg (0.19 mmol) of $[Mo(CO)_2(S_2C_2Me_2)_2]$ in 1 mL of THF. The dark green-brown solution was stirred for 2 h and filtered. The filtrate was taken to dryness to give a black solid, which was washed with ether (2×5 mL) and hexane (5 mL) and dissolved in a minimal volume of acetonitrile. Several volume equivalents of ether were added, and the solution was allowed to stand overnight. The product was isolated as 120 mg (82%) of dark green-brown crystals. IR (Nujol): ν_{CO} 1968 cm^{-1}. ^{1}H NMR (CD_3CN, anion): δ 1.01 (d, 12), 1.23 (d, 6), 2.50 (s, 12), 2.87 (septet, 1), 3.91 (septet, 2), 6.93 (s, 2). Absorption spectrum (acetonitrile): λ_{max} (ϵ_M) 323 (6910), 380 (6180), 474 (5450), 653 (1980) nm. Anal. Calcd. for $C_{32}H_{55}MoNOS_4Se$: C, 49.72; H, 7.17; N, 1.81; S, 16.59; Se, 10.22. Found: C, 49.63; H, 7.24; N, 1.79; S, 16.73; Se, 10.28.

$(Et_4N)[Mo(CO)(SeC_6H_2\text{-}2,4,6\text{-}Pr^i_3)(S_2C_2Ph_2)_2]$. The preceding method was followed but with use of $[Mo(CO)_2(S_2C_2Ph_2)_2]$. The product was isolated as dark green-brown crystals (85%). IR (Nujol): ν_{CO} 1942 cm^{-1}. ^{1}H NMR (CD_3CN, anion): δ 1.00 (d, 12), 1.22 (d, 6), 2.80 (septet, 1), 3.56 (m, 2), 6.84 (s, 2), 7.09 (m, 12), 7.25 (d, 8). Absorption spectrum (acetonitrile): λ_{max} (ϵ_M) 377 (15 800), 486 (9300), 643 (2980) nm.

X-ray Structure Determinations. The 13 compounds listed in Tables 1−3 were structurally characterized by X-ray crystallography. Component complexes are hereafter referred to by the numerical designations in Chart 1. Crystals of **1** and **16** were grown by slow evaporation of benzene solutions in the air. All other crystallizations were carried out anaerobically. Crystals of (Bu_4N)[**8**], (Bu_4N)[**12**], and (Et_4N)[**14**] were obtained from 5:1 acetonitrile/ether (v/v), and (Et_4N)[**5**] from 5:1 THF/ether (v/v). All other crystals were obtained by vapor diffusion where the first component specified is the parent solvent: $(Et_4N)_2$[**3**], (Et_4N)[**10**], $(Et_4N)_2$[**13**]·2MeCN·Et_2O, and (Et_4N)[**17**]·MeCN from acetonitrile/ether; (Et_4N)[**4**] from acetonitrile/Bu^{t}OMe; (Et_4N)[**9**] from THF/ether; $(Ph_4P)_2$[**7**]·2DMF from DMF/THF. Crystals were mounted on glass capillary fibers in grease and cooled in a stream of dinitrogen (−60 °C). Diffraction data were obtained with a Siemens (Bruker) SMART CCD area detector system using ω scans of 0.3 deg/frame with 30 or 60 s frames such that 1271 frames were collected for a hemisphere of data. The first 50 frames were recollected at the end of the data collections to monitor for crystal decay; no significant decay was observed. Cell parameters were determined using SMART software. Data reduction was performed with SAINT software, which corrects for Lorentz polarization and decay. Absorption corrections were applied by using the program SADABS as described by Blessing.[37] Space groups were assigned by analysis of symmetry and observed systematic absences determined by the program XPREP, and by successful refinement of the structure. All structures were solved by direct methods with SHELXS and subsequently refined against all data by the standard technique of full-matrix least-squares on F^2 (SHELXL-93,97).

Asymmetric units contain one (**1**, $(Et_4N)_2$[**3**], (Bu_4N)[**8**,**12**], (Et_4N)[**9**,**10**,**14**], $(Et_4N)_2$[**13**]·2MeCN·Et_2O, **16**, and (Et_4N)[**17**]·MeCN) or two ((Et_4N)[**5**]) formula weights, except for (Et_4N)[**4**] and $(Ph_4P)_2$[**7**]·2DMF, which contain half formula weight owing to an imposed 2-fold axis and an inversion center, respectively. The structure of (Et_4N)[**5**] was refined as a twinned monoclinic crystal which emulated the orthorhombic crystal system, and was modeled in SHELXTL-97 with a BASF value of 0.55. One methylene group and a methyl group of one of the cations in $(Et_4N)_2$[**13**]·2MeCN·Et_2O were disordered over two sites and were refined with site occupancy factors of 0.83 and 0.60, respectively. Carbon atoms of the cations in (Et_4N)[**4**] and (Et_4N)[**17**]·MeCN were disordered over two sites and were refined with occupancy factors of 0.51 and 0.68, respectively. All non-hydrogen atoms were described anisotropically. In the final stages of refinement, hydrogen atoms were added at idealized positions and refined as riding atoms with a uniform value of U_{iso}. Final refined structures were examined for any overlooked symmetry with the checking program PLATON. Crystallographic and final agreement factors are included in Tables 1−3. Metric parameters for the structures are collected in Tables 4−7. Because of the large quantity of data, mean values and ranges of values are given where feasible instead of individual data. (See the Supporting Information.)

Other Physical Measurements. Absorption spectra were recorded with a Perkin-Elmer Lambda 6 spectrophotometer. ^{1}H NMR spectra were recorded with a Bruker AM-500 spectrometer. IR spectra were measured with a Nicolet Impact 400 Fourier transform IR instrument. Cyclic voltammograms were recorded using a PAR Model 263 potentiostat/galvanostat with a Pt disk working electrode and 0.1 M $(Bu_4N)(PF_6)$ supporting electrolyte; potentials are referenced to the saturated calomel electrode (SCE).

(37) Blessing, R. H. *Acta Crystallogr.* **1995**, *A51*, 33.

Table 4. Bond Distances (Å) and Angles (deg) for Trigonal Prismatic Complexes **1**, **16**, and **17**

	1	**16**	**17**
Mo−S[a]	2.380(1)	2.377(5)	2.374(3)
C−S[a]	1.726(1)	1.714(9)	1.727(8)
C−C[a,b]	1.368(2)	1.357(5)	1.354(9)
Mo−C	2.025(3)		
C1−Mo−C2	83.5(1)		
S−Mo−S[c]	141.7(1), 148.1(1)	133.2(1)−138.6(1)	132.2(1)−137.4(1)
θ[d]	119.6	119.5−120.8	118.6−121.3
ϕ[a,e]		5.4	1.6

[a] Mean values. [b] Chelate ring. [c] Transoid angle, involving S atoms in different chelate rings. [d] Dihedral angle between MoS_2 planes. [e] Twist angle between opposite S_3 faces.

Table 5. Bond Distances (Å) and Angles (deg) for Complexes with Axial Oxygen Ligands **3**, **4**, and **5**

cluster	**3**	**4**	**5**
Mo−O1	1.712(2)	1.677(3)	1.867(8)
Mo−S[a]	2.388(1)	2.368(3)	2.32(1)
C−S[a]	1.783(3)	1.753(6)	1.77(4)
C−C[b]	1.328(6)[a]	1.327(5)	1.32(1)[a]
Mo−O1−C9			166.8(7)
δ[c]	0.765	0.773	0.825
θ[d]	129.7	128.5	125.7

[a] Mean values. [b] Chelate ring. [c] Perpendicular displacement of the Mo atom from S_4 least-squares plane. [d] Dihedral angle between MoS_2 planes.

Results and Discussion

In our most recent research on synthetic analogues of molybdoenzyme active sites,[23,24] we developed an efficient route to bis(dithiolene)$Mo^{IV}O$ complexes, among them the benzene-1,2-dithiolate complex $[MoO(bdt)_2]^{2-}$. This species proved to be a precursor to $[Mo^{IV}(OSiR_3)(bdt)_2]^{1-}$ and $[Mo^{VI}O_2(bdt)_2]^{2-}$ [24,38] by a silylation and an atom transfer reaction, respectively. The latter complex could be silylated to yield $[Mo^{VI}O(OSiR_3)(bdt)_2]^{1-}$. In these species, silyl oxide simulates serinate in an approach to DMSOR sites **a** and **b** (Figure 1). Analogous W(IV) complexes have also been prepared and shown to sustain oxo transfer reactions to $W^{VI}O$ products.[23,39] While these compounds are useful structural[40] and, to an extent, reactivity[24] analogues, they do not possess the dialkyldithiolene-type chelate ring of the pterin−dithiolene cofactor ligand.

Ligand System. To approach more closely the electronic situation in the chelate ring of the cofactor, we have turned to the nonaromatic ligand $R_2C_2S_2^{2-}$ with R = alkyl and phenyl. These ligands have not been isolated in substance, but their complexes are accessible by the methods outlined in Figure 2. Dicarbonyl precursor complexes **1** and **2** are synthesized by reaction 1, which is an improvement of the original method of

$$[Mo(CO)_3(MeCN)_3] + 2[Ni(S_2C_2R_2)_2] \rightarrow [Mo(CO)_2(S_2C_2R_2)_2] + [Ni^{II}{}_2(S_2C_2R_2)_2]_x + 3MeCN + CO \quad (1)$$

Schrauzer et al.[27] involving photolysis of a mixture of $[Mo(CO)_6]$ and $[Ni(S_2C_2R_2)_2]$. Yields are increased in our hands, and irradiation is not required. Red-violet **1** and blue-violet **2** are easily purified by column chromatography. An analogous procedure affords the complexes $[W(CO)_2(S_2C_2R_2)_2]$.[33] The structure of **1** is shown in Figure 3. The dihedral angle θ = 119.6° between MoS_2 planes and the S−Mo−S transoid angles of 142° and 148° (involving sulfur atoms in different chelate rings) (Table 4) reveal a close approach to trigonal prismatic (C_{2v}) stereochemistry, for which the ideal values are 120° and 136°, respectively. The average C−C distance of 1.368(2) Å is longer than a C=C double bond (1.33 Å), and the average C−S distance of 1.726(1) Å is shorter than a C−S single bond (1.82 Å), corresponding to an electron distribution intermediate between those of enedithiolate and dithione. As with the corresponding tungsten system,[33] reaction 1 can be interpreted as a four-electron oxidation of the metal by the transfer of two (neutral) dithione ligands from two $[Ni(S_2C_2R_2)_2]$ molecules. However, the molybdenum oxidation state in the product (Mo(II) or Mo(IV)) remains ambiguous. The corresponding expectation that **1** is redox-active is confirmed by two one-electron steps at −0.53 and −1.08 V in acetonitrile. Given that the R substituents in $[Mo(CO)_2(S_2C_2R_2)_2]$ are variable,[27,35] the synthetic approach in Figure 2 subsumes the classic dithiolene property of redox potential tunability.[25] This property may be of value in stabilizing certain types of molecules. The redox series $[M(CO)_2(S_2C_2R_2)_2]^z$ (M = Mo, W) will be described separately.[36] The reaction products of Figure 2 are considered in terms of the ligand type introduced by carbonyl substitution.

Oxo and Arene Oxide Ligation. The complexes are afforded in good yield by reaction 2 in THF and reaction 3 (R = Me, Ph) in acetonitrile.

$$[Mo(CO)_2(S_2C_2Me_2)_2] + 2OH^- \rightarrow [MoO(S_2C_2Me_2)_2]^{2-} + H_2O + 2CO \quad (2)$$

$$[Mo(CO)_2(S_2C_2R_2)_2] + ArO^- \rightarrow [Mo(OAr)(S_2C_2R_2)_2]^{1-} + 2CO \quad (3)$$

The Et_4N^+ salt of orange-brown oxo complex **3** precipitates from the reaction mixture of **1**, which always affords the blue-green byproduct $(Et_4N)_2[Mo(CO)_2(S_2C_2Me_2)_2]$. Complex **3** exhibits the standard square pyramidal stereochemistry shown in Figure 4 with θ = 130° and the molybdenum atom displaced from the S_4 plane by 0.77 Å (Table 5). The mean C−C (1.328(6) Å) and C−S (1.783(3) Å) bond lengths are indicative of an enedithiolate ligand description. Values of ν_{MoO} in KBr follow the trend **3** (889 cm^{-1}) < $[MoO(S_2C_2H_2)_2]^{2-}$ (904, 916 cm^{-1}) < $[MoO(S_2C_2(CN)_2)_2]^{2-}$ (932 cm^{-1}), consistent with Mo=O bond distances of 1.712(2) Å for **3** and 1.67(1) Å for the latter complex.[24] Evidently, as the electron-donating ability of the substituents increases, O → Mo electron donation decreases, leading to longer bonds and lower frequencies. Substituents have a marked effect on redox potentials for these and all other complexes examined in this work. As one example, three oxo complexes which support the three-membered electron-transfer series 4 are compared in Figure 5. Potentials occur in the order

$$[Mo^{IV}O(S_2C_2R_2)_2]^{2-} \leftrightarrow [Mo^{V}O(S_2C_2R_2)_2]^{1-} \leftrightarrow [Mo^{VI}O(S_2C_2R_2)_2] \quad (4)$$

$E_{1/2}$ (V) = −0.62/0.15 (R = Me), −0.46/0.29 (R = Ph), −0.08/0.54 (R = H,CN).[24] These data and the extensive tabulation given elsewhere[24] clearly reveal the substituent inductive effect on potentials. Of particular interest are $Mo^{VI}O$ species, the major portion of site **b**, which with **3** is accessible at a relatively low

(38) Ueyama, N.; Oku, H.; Kondo, M.; Okamura, T.; Yoshinaga, N.; Nakamura, A. *Inorg. Chem.* **1996**, *35*, 643.
(39) Lorber, C.; Donahue, J. P.; Goddard, C. A.; Nordlander, E.; Holm, R. H. *J. Am. Chem. Soc.* **1998**, *120*, 8102.
(40) Musgrave, K. B.; Donahue, J. P.; Lorber, C.; Holm, R. H.; Hedman, B.; Hodgson, K. O. *J. Am. Chem. Soc.* **1999**, *121*, 10297.

Table 6. Bond Distances (Å) and Angles (deg) for Bridged Binuclear Complexes **7** and **13**

	7	**13**		**7**	**13**
Mo1−Mo1A/2	3.024(1)	3.858(3)	C−C[a,b]	1.344(4)	1.338(4)
Mo1−S5/S5A	2.331(7), 2.339(7)		S−Mo−S/Se[c]	155.5(1)−158.9(1)	115.8(1)−148.3(1) Mo1[d]
Mo1−Se1		2.570(1)			127.0(1)−138.8(1) Mo2[d]
Mo1−Se2		2.680(1)	S5−Mo1−S5A	99.30(2)	
Mo2−Se1		2.569(1)	Mo1−S5−Mo1A	80.70(2)	
Mo2−Se2		2.648(1)	Se1−Mo1/2-Se2		70.18(3), 70.74(3)
Mo−S[a]	2.43(3)	2.33(1)	Mo1−Se1/Se2−Mo2		97.29(3), 92.77(3)
C−S[a]	1.736(5)	1.75(1)	θ[e]	84.9	124.2−129.1

[a] Mean values. [b] Chelate ring. [c] Range of transoid angles including bridge atoms. [d] Transoid angles not including bridge atoms: 132.3(1), 146.2(1) at Mo1; 137.7(1), 138.6(1) at Mo2. [e] Dihedral angle of MoS_2 (**7**) or MoS_2 and $MoSe_2$ planes (**13**) containing the same Mo atom.

Table 7. Bond Distances (Å) and Angles (deg) for Complexes with Thiolate (**8**, **9**, **10**) and Selenolate (**12**, **14**) Ligands

	8	**9**	**10**	**12**	**14**
Mo−S5/Se1	2.469(1)	2.338(1)	2.320(1)	2.585(1)	2.580(3)
Mo−S[a]	2.36(2)	2.31(7)	2.313(6)	2.36(2)	2.36(3)
Mo−C[a]	2.009(4)			1.99(1)	2.021(3)
C−S[a]	1.743(9)	1.763(7)	1.773(5)	1.73(3)	1.74(1)
C−C[a,b]	1.33(1)	1.322(1)	1.347(7)	1.343(2)	1.344(6)
C1−Mo−S5/Se1	78.94(9)			78.4(2)	81.53(8)
Mo−S5/Se1−C	110.1(1)	103.7(1)	102.6(1)	107.6(2)	108.4(1)
θ[c]	126.9	130.3	132.1	127.5	126.6
δ[d]		0.732	0.706		

[a] Mean values. [b] Chelate ring. [c] Dihedral angle between MoS_2 planes. [d] Perpendicular displacement of the Mo atom from the S_4 least-squares plane.

potential. The majority of $[Mo^{IV}O(S_2C_2R_2)_2]^{2-}$ complexes thus far examined show an irreversible second oxidation.[22,24] Complex **3** is readily oxidized by iodine to the blue-violet $Mo^{V}O$ species **4**, which has a very similar structure (not shown) with the expected marginally shorter bond lengths (Table 5).

Arene oxide complexes **5** and **6** were prepared by reaction 3 and isolated as orange- or red-brown Et_4N^+ salts. Hindered phenolate ligands were employed to suppress bridged dimer formation. The corresponding salt of $[Mo(OC_6H_2\text{-}2,4,6\text{-}Pr^i_3)(S_2C_2Me_2)_2]^{1-}$ proved difficult to obtain in pure form. The structure of **5** (Figure 4) is square pyramidal with an axial Mo−O bond length of 1.867(8) Å and an Mo−O−C angle of 166.8(7)°. Ligand dimensions again point to an enedithiolate formulation. The molecule is essentially isostructural with two $[Mo(OSiBu^tPh_2)(S_2C_2R_2)_2]^{1-}$ complexes described earlier.[24] Complexes **5** and **6** are extremely sensitive to air and traces of water, and must be handled accordingly to avoid the formation of **3** and other decomposition products. Both complexes exhibit the reversible three-membered electron-transfer series 5 (Figure 5)

$$[Mo^{III}(OAr)(S_2C_2R_2)_2]^{2-} \leftrightarrow [Mo^{IV}(OAr)(S_2C_2R_2)_2]^{1-} \leftrightarrow [Mo^{V}(OAr)(S_2C_2R_2)_2] \quad (5)$$

in which the two redox steps are separated by 2.0 V. The Mo(III) state is formed under highly reducing conditions ($E_{1/2}$ = −1.74 V (**6**), −1.95 V (**5**)), whereas the Mo(V) state is attainable under mildly oxidizing conditions ($E_{1/2}$ = 0.10 V (**5**), 0.30 V (**6**)). While these potentials do not relate directly to those obtained for the enzymes, the extremely negative values for the reduction of **5** and **6** offer one reason why Mo(III) is a highly improbable physiological oxidation level in DMSOR. These complexes are intended as approaches to native site **a**. The absorption spectrum of **5**, shown in Figure 6, exhibits features at λ_{max} (ϵ_M) = 336 (12 400), 411 (13 900), 475 (1630), 567 (530), and 724 (160) nm. With the exception of the 567 nm band, the spectrum is a red-shifted version of that of $[Mo(OSiBu^tPh_2)(bdt)_2]^{1-}$.[24] The intensities of the last two or perhaps three bands suggest assignment as d−d transitions. Apparently corresponding (but more intense) features in the spectrum of *Rs* DMSOR occur at 374, 430, and 640 nm,[1,41,42] but the precise correlation will depend on whether there is an undetected band that is the analogue of the 724 nm band of **5** beyond ca. 700 nm.

Sulfide and Thiolate Ligation. The first compounds sought in connection with terminal sulfur ligation were square pyramidal Mo^{IV}=S species. Hille[1] has noted the possible occurrence of the Mo=Q group (Q = S, Se) in oxidized members of the DMSOR family. We have shown that the complexes $[WQ(S_2C_2Ph_2)_2]^{2-}$ (Q = O, S, Se) are readily obtained from $[W(CO)_2(S_2C_2Ph_2)_2]$.[33] However, the analogous heterogeneous reaction of **1** with Na_2S in acetonitrile led to the isolation of only one product, dark green-blue **7** in low yield. The product was identified by an X-ray structure determination which, as shown in Figure 7, revealed it to be a centrosymmetric dimer with a planar $Mo^{V}_2(\mu\text{-}S)_2$ core and distorted octahedral coordination. It is isostructural with $[W_2(\mu\text{-}S)_2(S_2C_2Ph_2)_4]^{2-}$, which was prepared by chemical oxidation of $[WS(S_2C_2Ph_2)_2]^{2-}$,[33] and with $[Mo_2(\mu\text{-}S)_2(S_2C_2(CO_2Me)_2)_4]^{2-}$.[43] Bond distance and angle data are summarized in Table 6. The principal difference between the latter complex and **7** is that the Mo···Mo separation in **7** (3.024(1) Å) is 0.09 Å longer. This complex may be regarded as an oxidation product of putative $[MoS(S_2C_2Me_2)_2]^{2-}$. The oxidizing agent has not been identified.

In reactions with thiolate ligands, two different complexes have been isolated (Figure 2). Reaction 6 in THF (R = Me,

$$[Mo(CO)_2(S_2C_2R_2)_2] + ArQ^- \rightarrow [Mo(CO)_{2-n}(QAr)(S_2C_2R_2)_2]^{1-} + nCO \quad (6)$$

Ph; Q = S), in which the ligand is introduced directly or generated by reduction of the disulfide, affords complexes **8**−**10**. When benzenethiolate is used, the product is the dark green-brown monocarbonyl **8**. It was identified by the X-ray structure shown in Figure 8, which reveals that **8** is a distorted trigonal prismatic derivative of **1** (Table 7). The monocarbonyl is somewhat unstable in solution, decomposing to unidentified products. When subjected to irradiation to remove CO, **8** was converted to tris complex **17** (vide infra) and intractable oily byproducts. The complex was not decarbonylated at 50 °C in vacuo overnight.

Use of the larger 2,4,6-triisopropylbenzenethiolate ligand with **1** or **2** first generates the green-brown color characteristic of a

(41) Gruber, S.; Kilpatrick, L.; Bastian, N. R.; Rajagopalan, K. V.; Spiro, T. G. *J. Am. Chem. Soc.* **1990**, *112*, 8179.
(42) Bastian, N. R.; Kay, C. J.; Barber, M. J.; Rajagopalan, K. V. *J. Biol. Chem.* **1991**, *266*, 45.
(43) Coucouvanis, D.; Hadjikyriacou, A.; Toupadakis, A.; Koo, S.-M.; Ileperuma, O.; Draganjac, M.; Salifoglou, A. *Inorg. Chem.* **1991**, *30*, 754.

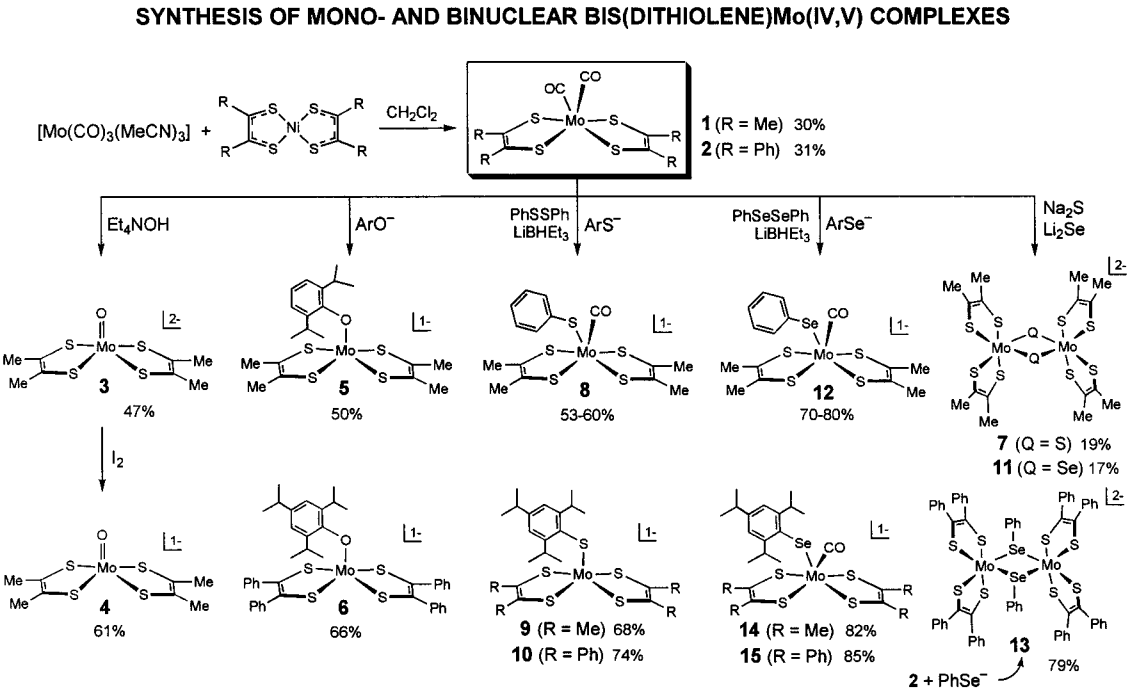

Figure 2. Scheme showing the synthesis of mono- and binuclear bis(dithiolene)molybdenum(IV,V) complexes **3**−**15** from dicarbonyl precursors **1** and **2**. Complexes **8** and **12** have been prepared by the two methods indicated (Ar = Ph); complexes **9**, **10**, **14**, and **15** were obtained using the reagent ArS^- or $ArSe^-$ (Ar = 2,4,6-triisopropylphenyl).

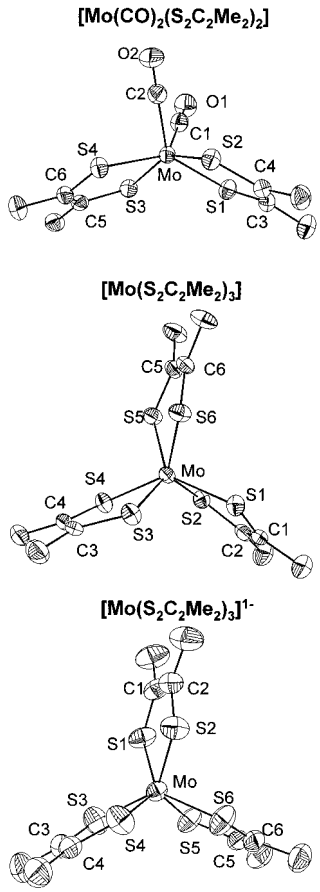

Figure 3. Structures of $[Mo(CO)_2(S_2C_2Me_2)_2]$ (top), $[Mo(S_2C_2Me_2)_3]$ (middle), and $[Mo(S_2C_2Me_2)_3]^{1-}$ (bottom), showing 50% probability ellipsoids and the atom labeling scheme.

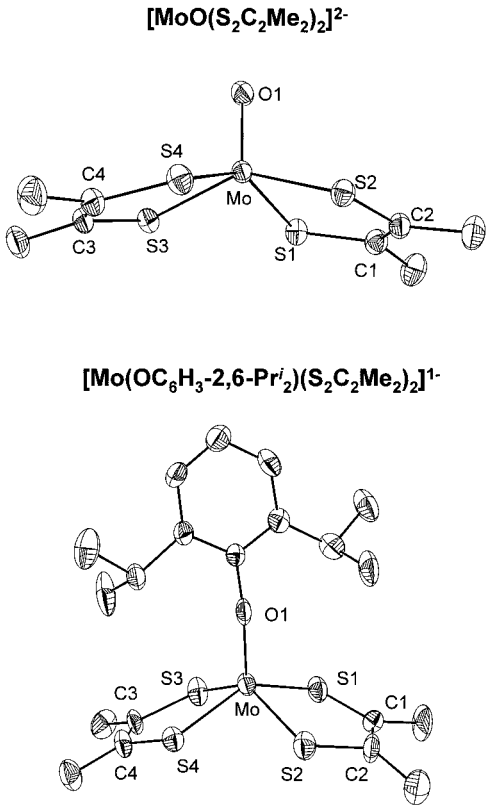

Figure 4. Structures of the complexes $[MoO(S_2C_2Me_2)_2]^{2-}$ (**3**, top) and $[Mo(OC_6H_3\text{-}2,6\text{-}Pr^i_2)(S_2C_2Me_2)_2]^{1-}$ (**5**, bottom) with axial oxygen ligands, showing 50% probability ellipsoids and the atom labeling scheme. The structure of $[MoO(S_2C_2Me_2)_2]^{1-}$ (**4**, not shown) is very similar to that of **3**.

monocarbonyl complex (detected by IR), followed by conversion to a red-brown solution from which **9** or **10** is isolated. The structures of these complexes are very similar (Table 7); that of **9** is presented in Figure 8. The molecule has the square pyramidal stereochemistry of **5** with enedithiolate ligands, Mo−SAr = 2.338(1) Å and Mo−S−C(Ar) = 103.7(1)°. Presumably, the steric bulk of the ligand and its mobility by rotation around

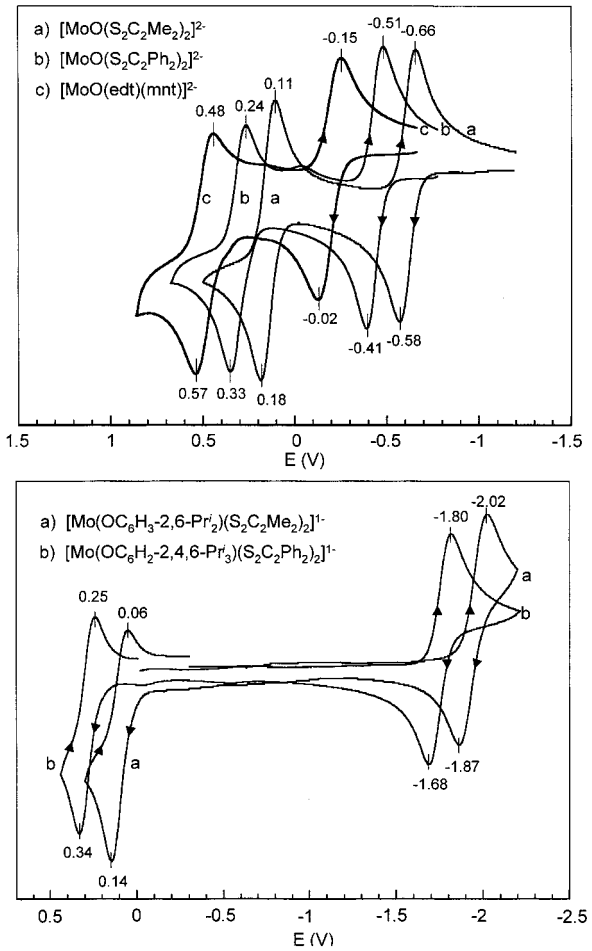

Figure 5. Cyclic voltammograms (100 mV/s) in acetonitrile solutions at 25 °C. Peak potentials vs SCE are indicated. Top: $[MoO(S_2C_2R_2)_2]^{2-}$, R = Me (**3**, a), Ph (b), H,CN (c). Bottom: $[Mo(OAr)(S_2C_2R_2)_2]^{1-}$, Ar = C_6H_3-2,6-Pr^i_2, R = Me (**5**, a); Ar = C_6H_2-2,4,6-Pr^i_3, R = Ph (**6**, b).

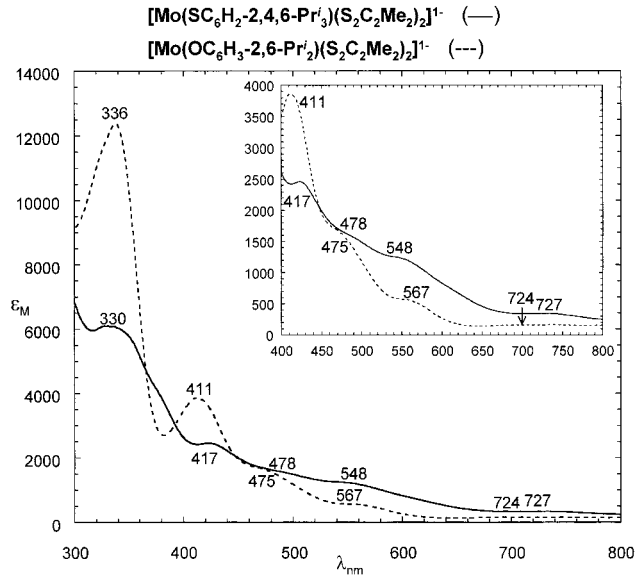

Figure 6. UV−vis spectra of $[Mo(OC_6H_3\text{-}2,6\text{-}Pr^i_2)(S_2C_2Me_2)_2]^{1-}$ (- - -) and $[Mo(SC_6H_2\text{-}2,4,6\text{-}Pr^i_3)(S_2C_2Me_2)_2]^{1-}$ (—) in THF. Band maxima are indicated.

the Mo−S and C−S bonds destabilizes carbonyl binding to the point where, under solvent removal in vacuo, CO is lost and **9** is obtained. In reaction 6 with R = Ph, the process is so fast that the solvent removal step is unnecessary to remove CO,

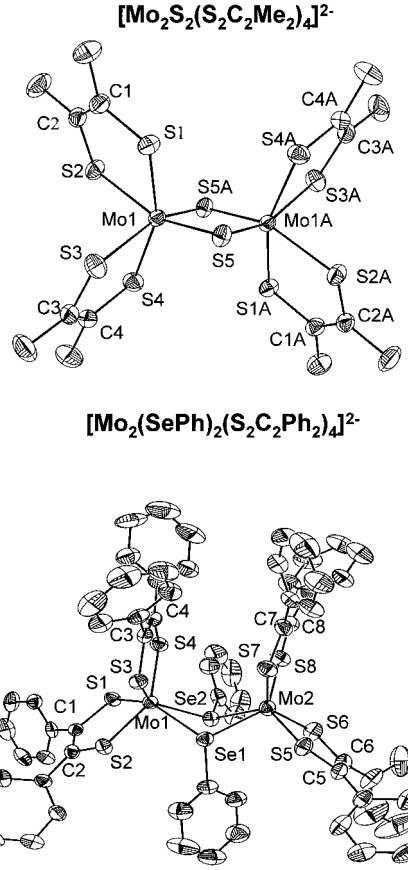

Figure 7. Structures of the binuclear complexes $[Mo_2(\mu\text{-}S)_2(S_2C_2\text{-}Me_2)_4]^{2-}$ (**7**, top) and $[Mo_2(\mu\text{-}SePh)_2(S_2C_2Ph_2)_4]^{2-}$ (**13**, bottom), showing 50% probability ellipsoids and the atom labeling scheme. Atoms labeled A are related to other atoms by an inversion center.

although it does improve the yield. Complexes **9** and **10** were prepared to simulate the ligand binding in dissimilatory nitrate reductase and in the Ser147Cys mutant of *Rs* DMSOR. The spectrum of **9** has a series of five bands that correlate with those in the spectrum of **5** (Figure 6). Three bands have been reported for mutant *Rs* DMSOR: λ_{max} (ϵ_M) 345 (8200), 415 (4200), 520 (4600) nm.[4] The first two bands may correspond to the 330 and 417 nm bands of **9**. The shoulder at 548 nm in the spectrum of **9** may correlate with the well-resolved 520 nm maximum in the mutant enzyme spectrum. However, band shapes are quite different, an observation that may relate to solvent and structural differences. No band assignments can be made here. However, complexes such as **5** and **9** should be useful objects for an ultimate interpretation of electronic spectral features of Mo(IV) enzyme states.

Selenolate Ligation. In this phase of the work, complexes with terminal selenide ligation, analogous to $[WSe(S_2C_2Ph_2)_2]^{2-}$,[33] were sought. The usual product from this reaction is dark green binuclear **11** in low yield. An isomorphous relationship between $(Ph_4P)_2$[**11**]·2DMF and the corresponding compound containing **7** is sufficient to characterize **11**. These complexes presumably form by oxidation to the Mo^VQ level followed by dimerization. Because neither **7** nor **11** is of direct interest relative to enzyme sites, we have not made a detailed attempt to identify the oxidant responsible for the Mo(V) state. However, the oxidation step is likely to be facile, given the low potential (−0.62 V) for the oxidation of $Mo^{IV}O$ complex **3** to **4** in series 4. Because both **7** and **11** were identified by X-ray analysis of selected crystals, the possibility of other products, including Mo═Q species, in the reaction systems **1**/Na_2S,Li_2Se remains.

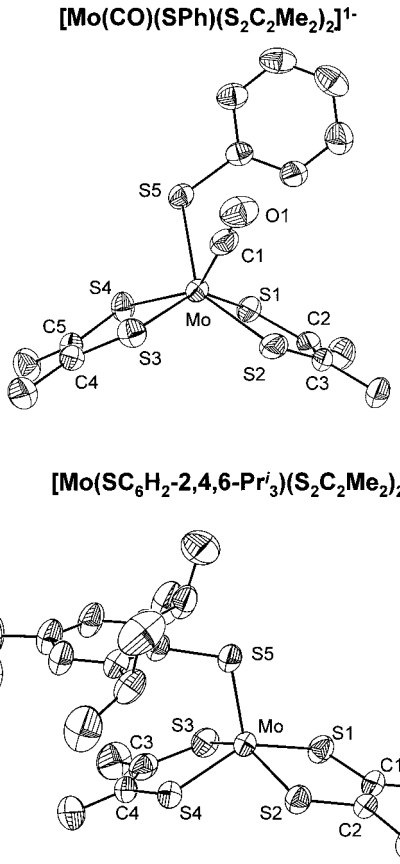

Figure 8. Structures of the thiolate complexes $[Mo(CO)(SPh)(S_2C_2Me_2)_2]^{1-}$ (**8**, top) and $[Mo(SC_6H_2\text{-}2,4,6\text{-}Pr^i_3)(S_2C_2Me_2)_2]^{1-}$ (**9**, bottom), showing 50% probability ellipsoids and the atom labeling scheme.

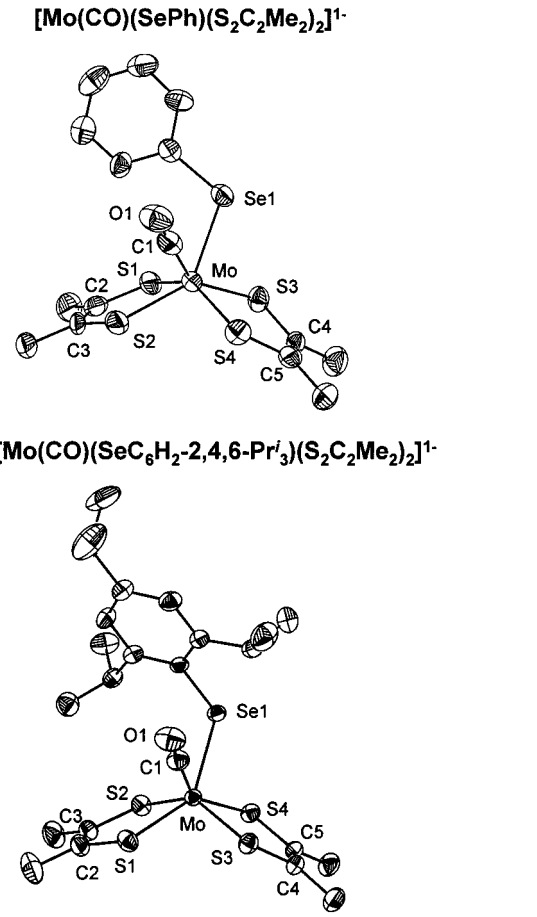

Figure 9. Structures of the selenolate complexes $[Mo(CO)(SePh)(S_2C_2Me_2)_2]^{1-}$ (**12**, top) and $[Mo(CO)(SeC_6H_2\text{-}2,4,6\text{-}Pr^i_3)(S_2C_2Me_2)_2]^{1-}$ (**14**, bottom), showing 50% probability ellipsoids and the atom labeling scheme.

Reactions of **1** and **2** with areneselenolates were carried out in the same manner as those with arenethiolates (Figure 2). However, the outcome was not always the same. Benzeneselenolate and **1** in reaction 6 (Q = Se) afforded dark green-brown **12**, completely analogous to thiolate complex **8**. Tetrabutylammonium salts are isomorphous (Tables 2 and 3), and the two complexes have the same distorted trigonal prismatic stereochemistry (Table 7) and essentially identical ν_{CO} values (1961 (**8**), 1956 (**12**) cm^{-1}). The structure of **12** is presented in Figure 9, with Mo−Se = 2.585(1) Å and Mo−Se−C = 107.6(2)°. The Mo−Se bond is 0.12 Å longer than the Mo−S bond in **8**. Other dimensions compared to those of **8** are not significantly different. Reaction 7 between **2** and benzeneselenolate took a different

$$2[Mo(CO)_2(S_2C_2Ph_2)_2] + 2PhSe^- \rightarrow [Mo_2(\mu\text{-}SePh)_2(S_2C_2Ph_2)_4]^{2-} + 4CO \quad (7)$$

course and resulted in formation of the brown Mo(IV) dimer **13**. This complex was identified by an X-ray structure determination, which reveals a nonplanar Mo_2Se_2 rhomboidal bridge with no metal−metal bonding (Mo···Mo = 3.858(3) Å) and severely distorted trigonal prismatic coordination at the molybdenum sites.

Having ascertained that benzeneselenoate and **1** or **2** did not produce five-coordinate species, reaction 6 with 2,4,6-triisopropylbenzeneselenolate was examined. Unlike the reaction systems with **1** or **2** and the corresponding thiolate, reaction 6 (Q = Se) afforded the monocarbonyl complexes **14** and **15** in good yield (Figure 2). The structure of **14** (Figure 9, Table 7) is distorted trigonal prismatic with Mo−Se = 2.580(3) Å and Mo−Se−C = 108.4(1)°. These values are indistinguishable from those of **12** and provide the only available indication in the complexes studied here that the large 2,4,6-triisopropylphenyl group does not introduce strain into the coordination unit, at least relative to the phenyl group. Heating in vacuo or photolysis has not as yet resulted in clean decarbonylation of **14** or **15**. Given the small range of ν_{CO} values for the Et_4N^+ salts of **12** (1945 cm^{-1}), **14** (1968 cm^{-1}), and **15** (1942 cm^{-1}), indicating energetically similar Mo−CO binding interactions, and essentially equal dihedral angles θ (Table 7), we are led to a conjecture. Is the 0.12 Å difference between Mo−Se and Mo−S bonds sufficient to diminish steric interactions between the hindered ligand and CO to the point where monocarbonyls **14** and **15** are substantially stable to decarbonylation? Given the existence of **9** and **10,** the differing decarbonylation tendencies of thiolate and selenolate complexes are unlikely to be related to the stability of the five-coordinate products. No intermediate carbonyl complex was observed in the formation of complexes **5** and **6**, where the axial Mo−O distance is only 1.87 Å in **5**. An analogue of site **e** of FDH presently remains unrealized and possibly will have to be attained by a route not involving carbonyl starting materials.

Tris(dithiolene) Complexes. In our synthetic and reactivity studies of dithiolene complexes,[24,33,39] we have frequently come across the complexes $[M(S_2C_2R_2)_3]^z$ (M = Mo, W) as byproducts or sometimes as reaction sinks. For example, we have encountered neutral green **16** in the preparation of **1** and blue monoanion **17** in the photolysis of **8**. We have determined their spectroscopic and electrochemical behavior, and have obtained them in crystalline form. The redox series $[Mo(S_2C_2Me_2)_3]^{0,1-,2-}$

with $E_{1/2} = -0.31$ and -0.94 V (vs Ag/AgCl) was described early in metal dithiolene research.[44] Definitive identification of **16** and **17** was obtained by structure determinations, the results of which are summarized in Figure 3 and Table 4. By the criteria of transoid S−Mo−S angle, twist angle ϕ, and dihedral angle θ, the two complexes closely approach the trigonal prismatic limit. Coordination geometries ranging between octahedral and trigonal prismatic are, of course, a common structural feature of tris(dithiolene) complexes. Pertinent examples include $[Mo(S_2C_2H_2)_3]$,[45] $[Mo(bdt)_3]$,[46] $[Mo(S_2C_2(COOMe)_2)_3]^{2-}$,[47] $[Mo(qdt)_3]$,[1−,2−,48,49] and $[Mo(mnt)_3]^{2-}$.[50]

Summary. The following are the principal results and conclusions of this investigation:

(1) Bis(dithiolene)dicarbonyl complexes $[Mo(CO)_2(S_2C_2R_2)_2]$ (R = Me, Ph) are obtainable in ca. 30% yield by the thermal reaction of $[Mo(MeCN)_3(CO)_3]$ and $[Ni(S_2C_2R_2)_2]$. These species serve as direct precursors by carbonyl substitution reactions to 12 mononuclear and binuclear complexes containing the $Mo(S_2C_2R_2)_2$ unit (Figure 2). All key complexes have been characterized by X-ray structure determinations. The immediate targets of this work are analogues of reduced enzyme sites **a**, **c**, and **e** in the DMSOR family of enzymes (Figure 1).

(2) $[Mo(CO)_2(S_2C_2Me_2)_2]$ undergoes rapid carbonyl displacement with Et_4NOH and Na_2S/Li_2Se to afford square pyramidal $[MoO(S_2C_2Me_2)_2]^{2-}$ and binuclear $[Mo_2(\mu\text{-}Q)_2(S_2C_2Me_2)_4]^{2-}$ (Q = S/Se), respectively.

(3) Reaction of **1** and **2** with large ArO^- ligands gives square pyramidal $[Mo(OAr)(S_2C_2R_2)_2]^{1-}$ which, together with $[Mo(OSiR'_3)(bdt)_2]^{1-}$ and $[Mo(OSiR'_3)(S_2C_2H_2)_2]^{1-}$,[24] provides structural analogues of the $[Mo^{IV}(O\cdot Ser)(S_2pd)_2]$ site (**a**) of *Rs* DMSOR. These complexes and site **a** exhibit similarities in absorption spectra.

(4) In reactions similar to reaction 3 with thiolate and selenolate ligands PhQ^- and sterically bulky ArQ^-, distorted trigonal prismatic $[Mo(CO)(QPh)(S_2C_2Me_2)_2]^{1-}$ and $[Mo(CO)(QAr)(S_2C_2R_2)_2]^{1-}$ (Q = S, Se) and square pyramidal $[Mo(SAr)(S_2C_2R_2)_2]^{1-}$ are obtained. The latter is a structural analogue of $[Mo^{IV}(S\cdot Cys)(S_2pd)_2]$ sites **c** of a dissimilatory nitrate reductase and a mutant DMSOR. Monocarbonyl thiolate and selenolate complexes differ in their decarbonylation properties; consequently, the species $[Mo(SeAr)(S_2C_2R_2)_2]^{1-}$, a possible analogue of site **e** of FDH, has not yet been obtained.

(5) Certain complexes in reactions 3 and 6 are intended as analogues of metal sites in the DMSOR family. They are *structural* analogues in which the dithiolene ligands simulate tight, symmetrical chelation by the pterin−dithiolene cofactor, and the axial ligands ArQ^- (Q = O, S), although aromatic, approximate serinate or cysteinate binding. Bond distances indicate that the dithiolene ligands function as (innocent) ene-1,2-dithiolates, the expected situation in enzyme sites. The stability of monocarbonyls such as $[Mo(CO)(QPh)(S_2C_2Me_2)_2]^{1-}$ raises the possibility of CO binding in the reduced forms of certain enzymes.

This research provides the initial definition of the types and structures of reduced bis(dithiolene)molybdenum complexes accessible through dicarbonyls **1** and **2**. Future work will build upon these results by an investigation of the XAS and electron and atom transfer reactivity properties of analogue complexes, including attempts to achieve Mo(VI) sites (Figure 1).

Acknowledgment. This research was supported by NSF Grant CHE 95-23830. We thank Drs. C. A. Goddard and C. Lorber for experimental assistance and useful discussion.

Supporting Information Available: X-ray crystallographic files in CIF format for the structure determinations of the 13 compounds in Tables 1−3. This material is available free of charge via the Internet at http://pubs.acs.org.

IC9908672

(44) Olson, D. C.; Mayweg, V. P.; Schrauzer, G. N. *J. Am. Chem. Soc.* **1966**, *88*, 4876.
(45) Smith, A. E.; Schrauzer, G. N.; Mayweg, V. P.; Heinrich, W. *J. Am. Chem. Soc.* **1965**, *87*, 5798.
(46) Cowie, M.; Bennett, M. J. *Inorg. Chem.* **1976**, *15*, 1584.
(47) Draganjac, M.; Coucouvanis, D. *J. Am. Chem. Soc.* **1983**, *105*, 139.
(48) Boyde, S.; Garner, C. D.; Enemark, J. H.; Ortega, R. B. *J. Chem. Soc., Dalton Trans.* **1987**, 297.
(49) Boyde, S.; Garner, C. D.; Enemark, J. H.; Bruck, M. A.; Kristofzski, J. G. *J. Chem. Soc., Dalton Trans.* **1987**, 2267.
(50) Brown, G. F.; Stiefel, E. I. *Inorg. Chem.* **1973**, *12*, 2140.